JOURNAL OF AGRICULTURAL AND FOOD CHEMISTRY

Functional Structure/Activity Relationships

Synthesis, optimization, and evaluation of glycosylated naphthalimide derivatives as efficient and selective insect #-N-acetylhexosaminidase OfHex1 inhibitors

Shengqiang Shen, Lili Dong, wei chen, renjie wu, Huizhe Lu, Qing Yang, and Jianjun Zhang

J. Agric. Food Chem., **Just Accepted Manuscript** • DOI: 10.1021/acs.jafc.9b02281 • Publication Date (Web): 15 May 2019

Just Accepted

ACS Publications

is published by the American Chemical Society. 1155 Sixteenth Street N.W., Washington, DC 20036

Synthesis, optimization, and evaluation of glycosylated naphthalimide derivatives as efficient and selective insect β-N-acetylhexosaminidase OfHex1 inhibitors

Shengqiang Shen,[†,#] Lili Dong,[†,#] Wei Chen,[‡] Renjie Wu,[†] Huizhe Lu,[†] Qing Yang,*[,‡] and Jianjun Zhang*[,†]

[†]Department of Applied Chemistry, College of Science, China Agricultural University, Beijing, China

[‡]Institute of Plant Protection, Chinese Academy of Agricultural Sciences, Beijing 100193, China

ABSTRACT: Insect chitinolytic β-*N*-acetylhexosaminidase OfHex1, from the agricultural pest *Ostrinia furnacalis* (Guenée), is considered as a potential target for green pesticide design. In this study, rational molecular design and optimization led to the synthesis of compounds **15r** (K_i =5.3 μM) and **15y** (K_i =2.7 μM) that had superior activity against OfHex1 than previously reported lead compounds. Both **15r** and **15y** had high selectivity towards OfHex1 over HsHexB (human β-*N*-acetylhexosaminidase B) and hOGA (human O-GlcNAcase). In addition, to investigate the basis for the potency of glycosylated naphthalimides against OfHex1, molecular docking and MD simulations were performed to study possible binding modes. Furthermore, the *in vivo* biological activity of target compounds with efficient OfHex1 inhibitory potency were assayed against *Myzus persicae*, *Plutella xylostella*, and *Ostrinia furnacalis*. This present work indicates that glycosylated naphthalimides can be further developed as potential pest control and management agents targeting OfHex1.

KEYWORDS: Glycosylated naphthalimids, β-N-acetylhexosaminidase, OfHex1, inhibitors, molecular

21 docking, MD simulations

22 **INTRODUCTION**

23 Chitin is a homopolymer of β-1,4-linked *N*-acetyl-β-D-glucosamine (GlcNAc), and is the second most
24 abundant polysaccharide in nature.[1] Chitin is also a key structural component of the fungal cell wall, nematode
25 eggshell, and arthropod exoskeleton.[2] Moreover, the cuticles of the integument and peritrophic membranes of
26 the midgut have found to contain chitin.[3] Chitin degradation is catalyzed by two members of the glycoside
27 hydrolase family, GH18 chitinases (EC 3.2.1.14) and GH20 β-*N*-acetylhexosaminidases (EC 3.2.1.52).[4,5]
28 GH18 chitinases catalyze the cleavage of chitin into shorter chito-oligosaccharides, then GH20
29 β-*N*-acetylhexosaminidases hydrolyze these oligosaccharides into *N*-acetyl-D-glucosamine (GlcNAc) from
30 terminal non-reducing.[4,5] Chitin degradation is essential to the growth and maturation of insects.[6,7] Interference
31 with insect chitin degradation disrupts molting, pupation and eclosion processes, eventually leading to insect
32 death.[6,8] Chitin is completely absent from higher plants and mammals,[5] and thus the inhibition of chitin
33 degradation is a promising strategy for the development of green pesticides.[5-10]

34 GH20 β-*N*-acetylhexosaminidase OfHex1 from the destructive agricultural pest, *Ostrinia furnacalis*
35 (Guenée), is an important enzyme during insect chitin degradation.[11] The physiological function of OfHex1
36 shown via RNA interference is to degrade of old cuticles of *O. furnacalis*.[12] Furthermore, the crystal structure
37 of OfHex1 (PDB: 3NSM) revealed the unique structural feature, with long substrate-binding pocket containing
38 two subsites (-1 and +1).[11] The -1 subsite is responsible for catalysis substrates, whilst the +1 subsite is
39 responsible for binding related moieties of substrates to enhance affinity and specificity.[11,12] The
40 crystallography of OfHex1 has attracted intense research attention and provides a solid foundation for the
41 design of specific inhibitors.[10,13-15]

42 To date, a number of OfHex1 inhibitors have been reported, including TMG-chitotriomycin[12], PUGNAc[9],
43 NAG-thiazoline (**NGT**)[13], naphthalimides[14-15], phlegmacin B1[7], berberine[16], thiazolylhydrazones[10]. Among
44 these inhibitors, NAG-thiazoline is the only molecule designed as an analog of the oxazolinium reaction
45 intermediate, but shows poor potency against OfHex1 with K_i values of 79 μM.[13] Subsequently, **NMAGT**
46 bearing a methylamino substituent on the thiazoline ring was designed and synthesized by Yang, and exhibited
47 higher inhibitory activity (K_i value of 0.13 μM) against OfHex1.[13] This suggested that the enlargement of the
48 functional group on the thiazoline could improve inhibitory activity against OfHex1. Naphthalimide
49 derivatives, including **Q1** and **Q2**, are an important class of non-carbohydrate inhibitors of OfHex1.[14] In
50 particular, **Q1** has been shown to exhibit inhibitory activity towards OfHex1 with a K_i value of 4.28 μM.[14] **Q2**
51 containing a dimethylamino group at the naphthalimide exhibited a K_i value of 0.31 μM against OfHex1.[14] The
52 complex crystal structures of **Q1**-OfHex1 (PDB: 3WMB) and **Q2**-OfHex1 (PDB: 3WMC) show that the
53 thiadiazole moiety bound the -1 subsite of the active pocket, and that the naphthalimide group was sandwiched
54 by residues Val327 and Trp490 at the +1 subsite.[14] In addition, related to the naphthalimide moiety of **Q1** in
55 OfHex1, the 4-dimethylaminonaphthalimide of **Q2** rotates approximately 180° to Trp490.[14] This
56 conformational change ultimately results in tight binding of **Q2** to OfHex1, leading to a 13-fold increase in
57 potency compared with **Q1**.[14] Thus, the 4-substituent at the naphthalimide group exerts a critical effect on the
58 potency against OfHex1(Figure 1).

59 In our previous studies, we presented glycosylated naphthalimide derivatives as promising lead compounds
60 for β-*N*-acetyl-D-hexosaminidase inhibitors.[15,17,18] In particular, inhibitors **15k**[17] (**1**, K_i =16.3 μM, unpublished
61 data), **6e**[15] (**2**, K_i =22.4 μM, unpublished data), and **6f** [15] (**3**, K_i =21.8 μM) exhibited higher inhibitory potency
62 towards OfHex1. Considering the crucial roles of OfHex1 to agricultural pest control, we further modified

these structures to improve the inhibitory efficiency. Prompted by these observations, we retained the frame structure of glycosylated naphthalimides and focused on two aspects of optimization, namely the 2-acetamido group at the glycosyl moiety (to increase affinity at the -1 the subsite) and the 4-substituent at the naphthalimide (to increase affinity at the +1 subsite) (Figure 1). Accordingly, several classes of glycosylated naphthalimide derivatives were synthesized and the inhibitory activity against OfHex1 was evaluated. To investigate the selectivity of these naphthalimides, their inhibitory capabilities towards human β-*N*-acetylhexosaminidase B (HsHexB) and human O-GlcNAcase (hOGA) were assessed. This work may provide useful information for future design of eco-friendly pesticides.

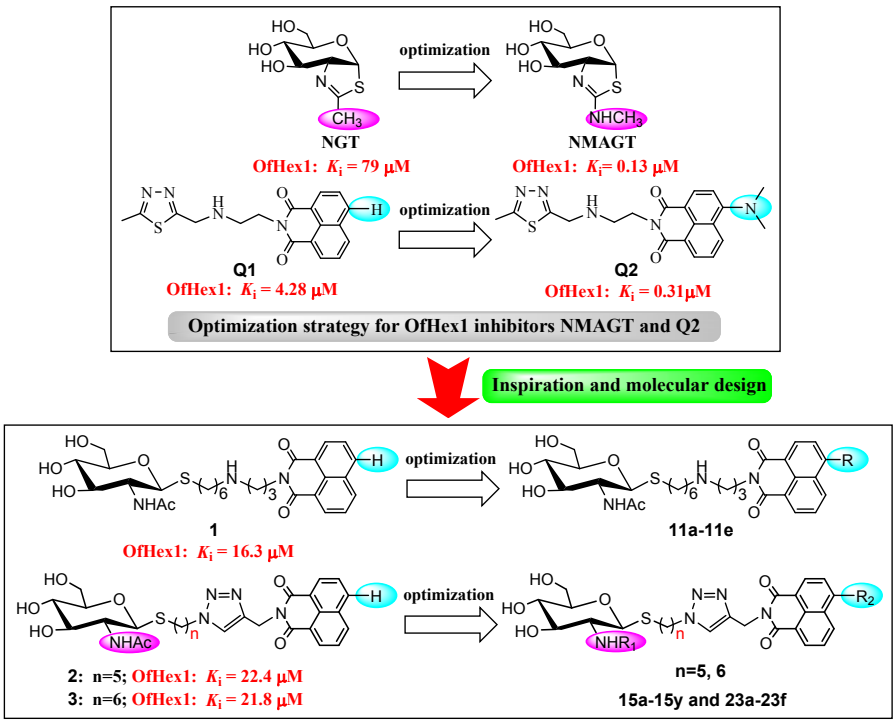

Figure 1. Design of novel glycosylated naphthalimide derivatives for OfHex1.

MATERIALS AND METHODS

Materials. All commercial materials were commercially available and treated with standard methods before use. With TMS as an internal reference, a Bruker AVANCE600 spectrometer was used to record ^{1}H NMR-300

76 MHz and ^{13}C NMR-75 MHz in $CDCl_3$ or DMSO-d_6 at 25°C. The Bruker Daltonics Bio-TOF-Q III mass
77 spectrometer (Bruker Co., Karlsruhe, Germany) was used to give high-resolution mass spectra (HRMS).
78 Reaction progress was monitored using thin layer chromatography (TLC) on silica gel GF254 plates with
79 detection by charring with 15% (v/v) H_2SO_4 in MeOH or by UV light (254 nm).

80 **Synthetic Chemistry.** Detailed synthetic procedures and characterization data for all of the synthesized
81 compounds are given in the Supporting Information.

82 **Enzyme Preparation.** OfHex1 was overexpressed in *Pichia pastoris* and then purified according to
83 previous methods.[12] HsHexB was obtained as described in the literature.[17] Human O-GlcNAcase (hOGA) was
84 overexpressed in *Escherichia coli* BL21(DE3) and purified by IMAC as described previously.[19]

85 **Enzyme Inhibitory Activity Assays.** The inhibitory activities of OfHex1, HsHexB, and hOGA were
86 assayed in end-point experiments using 4-methylumbelliferyl N-acetyl-β-D- glucosaminide (4-MU-GlcNAc)
87 as the substrate. OfHex1 and hOGA were assayed in 20 mM sodium phosphate buffer (pH 6.5), HsHexB was
88 assayed in 20 mM sodium citrate buffer (pH 4.5). In a final assay volume of 100 μL, the enzyme was
89 pre-incubated with inhibitors in buffer for 10 min at 30 °C, then 40 μM substrate (4-MU-GlcNAc) was added.
90 After incubation for a further 20 min at 30 °C, the reaction was terminated by the addition of 100 μl 0.5 M
91 sodium carbonate solution. The fluorescence of the liberated MU was quantitated using a Varioskan Flash
92 microplate reader (Thermo Fisher Scientific, Waltham, MA, USA) at an excitation of 366 nm and emission of
93 445 nm. When determining the IC_{50} values, various inhibitor concentrations were used to detect the
94 corresponding inhibition rates. The inhibition constant (K_i) was obtained using Dixon plots by changing the
95 concentration of the 4-MU-GlcNAc at a constant concentration (40, 20 and 10 μM).

96 **Molecular Docking.** The crystal structure of OfHex1 in complex with PUGNAc (PDB ID:3OZP)[9] was

97 retrieved from the Protein Data Bank and used as the starting model for molecular docking employing the
98 Sybyl Software (Version 7.3).[20] Prior to docking calculations, the structures were optimized using MMFF94
99 force field. For the protein, all water molecules were removed and missing hydrogen atoms were added.
100 Subsequently, the ligand protomol, appropriate putative ligand pose, was generated by ligand mode based on
101 the Hammerhead scoring function with the molecular similarity algorithm in the active domain of the
102 receptor.[21-23] Finally, molecular dockings were performed using the Surflex–Dock algorithm.

103 **Molecular Dynamics (MD) Simulations.** To obtain the convincing conformations, the molecular dynamics
104 (MD) simulations were carried out after docking. MD simulations of three systems (OfHex1 in complex with
105 ligands **15r**, **15y**, and **23f**) were performed using the Amber14 package[24]. AMBER03 force field[25] was selected
106 for the protein, and GAFF force field[26] was selected for the ligand. Each system was immersed in a truncated
107 octahedral box with TIP3P water molecules and electrostatic neutralized by adding appropriate number of
108 counterions (Cl^- or Na^+). Initially, Sander module was used to realize the energy minimization of the system.
109 The hydrogen atoms and water molecules were minimized with the 2500 cycles of steepest descent followed
110 by the conjugated-gradient methods. Then, 2500 cycles of the steepest-descent and 2500 cycles of the
111 conjugated gradient algorithm were carried out to minimize all atoms of the systems. After that, the system
112 was heated gradually from 0 to 300 K in the NVT ensemble and equilibrated in 300 K. Finally, MD
113 Simulations of 30 ns were performed at a constant temperature of 300 K and pressure of 1 atm employing the
114 PMEMD module. The SHAKE method[27] was applied to constrain hydrogen atoms, and the particle mesh
115 Ewald (PME) method[28] was used to treat the long-range electrostatic interactions under periodic boundary
116 conditions.

117 **In Vivo Activity.** Target compounds that efficiently inhibited OfHex1 were further tested for their

118 insecticidal activity against *Myzus persicae* and *Plutella xylostella* according to previous studies.[29-30] Test
119 compounds were dissolved in DMSO and diluted to a final concentration of 600 μg/mL and 200 μg/mL.
120 Hexaflumuron was used as a positive control and DMSO was used as a negative control. *Myzus persicae* and
121 *Plutella xylostella* were treated for 48h and 72h, respectively. Each bioassay was repeated in triplicate.

122 *Ostrinia furnacalis* larvae were raised using an artificial diet with a relative humidity of 70% at 26−28 °C.
123 Day 1 third-instar larvae were selected for feeding experiments. Compounds **15r** and **15y** were dissolved in
124 DMSO and diluted with an artificial diet to a final concentration of 600 μg/mL. In the control group, the
125 artificial diet contained an equal volume of DMSO. Each group contained 30 individual larvae that were
126 continuously fed for 5 days.[7,16]

127 **RESULTS AND DISCUSSION**

128 **Synthesis of Target Compounds 11a-11e and 15a-15t.** The target compounds **11a-11e** are outlined in
129 Scheme 1. Briefly, the key intermediates **6a-6e**[18,31] and **9b**[17] were obtained according to published methods
130 (Schemes S1-S3). Treatment of **9b** with excess naphthalimides **6a-6e** in the presence of K_2CO_3 and CH_3CN
131 yielded the acetyl-protected compounds **10a-10e**. The deacetylation of **10a-10e** via methanol-ammonia
132 catalysis resulted in **11a-11e** (Scheme S3).

133 To investigate the influence of the 2-substituent group (at glycosyl moiety) and the 4-substituent group (at
134 naphthalimide) on the inhibitory activity and selectivity against OfHex1, triazole group-bearing
135 thioglycosyl-naphthalimides **15a-15t** were synthesized (Scheme 2). Bromides **9a-9d** were prepared according
136 to literature procedures[15], which on further reaction with NaN_3 yielded key intermediates **13a-13d** (Scheme
137 S6). Meanwhile, naphthalimide derivatives **12a-12e** were prepared as previously reported[15,32] (Schemes
138 S4-S5). Subsequently, azides **13a-13d** were reacted with **12a-12e** in 2:1 THF/water mixture via Cu-catalyzed

139 cycloaddition to form precursors **14a-14t**. Finally, deprotection of **14a-14t** was performed using

140 methanol-ammonia to produce the target compounds **15a-15t** (Scheme S6).

141

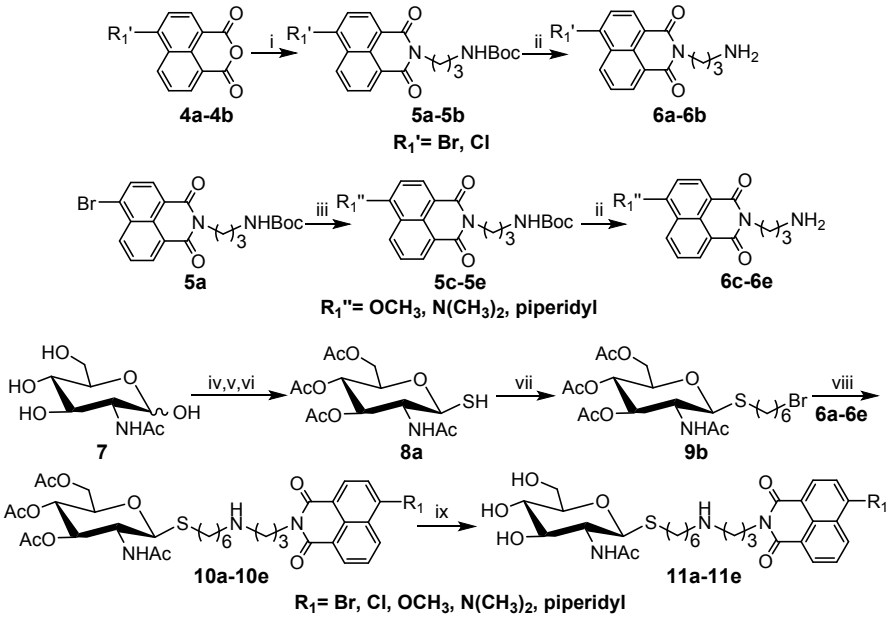

142

143

144 **Scheme 1.** Synthesis of glycosylated naphthalimide derivatives **11a-11e**. (i) *tert*-butyl (3-aminopropyl) carbamate, EtOH; (ii)

145 DCM, CF_3COOH; (iii) MeOH, KOH for **5c**; dimethylamine, 2-methoxyethanol for **5d**; piperidine, 2-methoxyethanol for **5e**; (iv)

146 AcCl; (v) thiourea, acetone; (vi) $Na_2S_2O_5$, DCM, H_2O; (vii) 1,6-dibromohexane, K_2CO_3, acetone, H_2O; (viii) **6a-6e**, K_2CO_3,

147 CH_3CN; (ix) NH_3, MeOH.

148

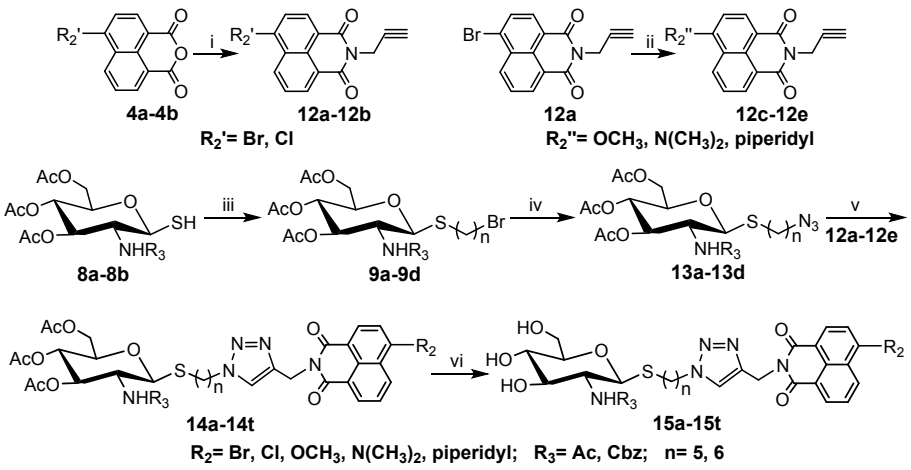

Scheme 2. Synthesis of glycosylated naphthalimide derivatives **15a-15t**. (i) 2-propynylamine, EtOH; (ii) MeOH, KOH for **12c**; dimethylamine, 2-methoxyethanol for **12d**; piperidine, 2-methoxyethanol for **12e**; (iii) a, ω- dibromoalkane, K_2CO_3, acetone, H_2O; (iv) NaN_3, K_2CO_3, acetone, H_2O; (v) **12a-12e**, $CuSO_4$, sodium ascorbate, THF, H_2O; (vi) NH_3, MeOH.

Evaluation of Enzyme Inhibitory Activity. The target compounds **11a-11e** and **15a-15t** were evaluated for their inhibitory activity against OfHex1, HsHexB, and hOGA (Tables 1-3).

As shown in Table 1, the substituents at the 4-position of naphthalimide moiety (**11a-11e**) improved the inhibitory potency against OfHex1 compared to naphthalimide bearing no 4-substituent group (compound **1**). In particular, naphthalimides **11a-11c** bearing smaller functional groups (Br, Cl, OMe) exhibited a minor increase in activity. Naphthalimides **11d-11e** bearing a basic substituent ($N(CH_3)_2$ or piperidyl) resulted in a more effective inhibitory potency. Among these inhibitors, compound **11d** bearing the dimethylamino group showed the highest inhibitory activity against OfHex1 with an IC_{50} value of 13.4 μM (Table 3). Additionally, **11d** showed no inhibitory activities against HsHexB and hOGA, which exhibited improved selectivity compared to lead compound **1**.

As shown in Table 2, bioassay results of **15a-15t** revealed that 2-substituent of the glycosyl moiety and 4-substituent of naphthalimide significantly influenced the potency and selectivity of these compounds

165 towards OfHex1. Specifically, upon increasing the size from acetyl (Ac) to benzyloxycarbonyl (Cbz), a loss in
166 inhibitory activity against OfHex1 was observed. These results suggest that a large substituent at the 2-position
167 of the sugar ring leads to steric hindrance, ultimately decreasing the binding affinity of the inhibitors and
168 OfHex1. The 4-substituted group on naphthalimide moiety increased the inhibitory potency against OfHex1
169 compared to lead compounds **2** and **3**. In detail, inhibitors bearing 4-bromo (**15a-15b**) and 4-piperidyl
170 (**15q-15r**) groups possessed improved potency towards OfHex1 compared to inhibitors bearing Cl (**15e-15f**),
171 OCH_3 (**15i-15j**), and $N(CH_3)_2$ (**15m-15n**) substituents. The length of the linker between glycosyl and triazole
172 also affected the activity against OfHex1, and increasing the length of the carbon atoms from five to six
173 slightly increased their activity (e.g. **15b**>**15a** or **15r**>**15q**). Further IC_{50} determination showed that **15r** had
174 the highest inhibitory potency against OfHex1 (IC_{50} = 6.4 μM) in **15a-15t** and more selective than lead
175 compounds **2** and **3** (Table 3).

176

177 **Table 1. Inhibition rates of 11a-11e against OfHex1, HsHexB, and hOGA at 10 μM.**

178

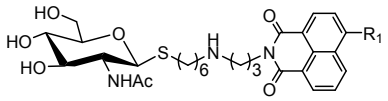

Compd	R_1	Inhibition rate at 10 μM (%)		
		OfHex1	HsHexB	hOGA
11a	Br	39.6 ± 3.1	13.9 ± 0.6	21.0 ± 0.5
11b	Cl	46.0 ± 1.8	9.2 ± 0.2	18.3 ± 2.2
11c	OMe	42.6 ± 1.6	12.5 ± 1.1	7.7 ± 1.6
11d	$N(CH_3)_2$	**54.6 ± 0.8**	**13.9 ± 1.7**	**12.7± 0.3**

11e	piperidyl	48.3 ± 0.7	13.6 ± 0.5	14.2 ± 0.8
1	H	35.2 ± 1.7	20.1 ± 0.1	9.9 ± 0.3

179

180 **Table 2. Inhibition rates of 15a-15t against OfHex1, HsHexB, and hOGA at 10 μM.**

181

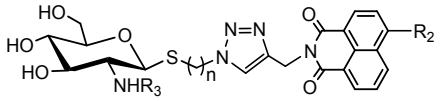

Compd	substituent group			Inhibition rate at 10 μM (%)		
	R_2	R_3	n	OfHex1	HsHexB	hOGA
15a	Br	Ac	5	66.0 ± 1.3	11.2 ± 1.4	14.1 ± 0.5
15b	Br	Ac	6	68.1 ± 2.5	6.7 ± 0.8	17.6 ± 0.3
15c	Br	Cbz	5	8.7 ± 1.2	7.9 ± 0.1	4.0 ± 0.4
15d	Br	Cbz	6	15.3 ± 3.6	7.4 ± 0.3	13.0 ± 0.5
15e	Cl	Ac	5	37.6 ± 1.5	10.1 ± 1.8	11.4 ± 0.7
15f	Cl	Ac	6	49.2 ± 2.8	10.3 ± 2.0	17.8 ± 0.3
15g	Cl	Cbz	5	19.6 ± 2.6	4.8 ± 0.7	7.3 ± 1.2
15h	Cl	Cbz	6	11.2 ± 1.3	3.7 ± 0.8	10.9 ± 0.4
15i	OMe	Ac	5	42.2 ± 2.9	10.5 ± 0.4	11.5 ± 0.6
15j	OMe	Ac	6	60.1 ± 0.6	8.0 ± 1.1	13.8 ± 0.5
15k	OMe	Cbz	5	19.6 ± 1.4	2.1 ± 1.5	7.2 ± 0.9
15l	OMe	Cbz	6	11.2 ± 3.0	12.4 ± 0.2	10.9 ± 0.8
15m	$N(CH_3)_2$	Ac	5	56.9 ± 0.5	8.1 ± 0.3	13.1 ± 0.8

15n	$N(CH_3)_2$	Ac	6	57.9 ± 2.1	9.7 ± 0.9	13.3 ± 0.2
15o	$N(CH_3)_2$	Cbz	5	24.2 ± 2.4	9.3 ± 0.7	8.2 ± 0.5
15p	$N(CH_3)_2$	Cbz	6	19.7 ± 1.7	6.1 ± 1.9	10.9 ± 0.7
15q	piperidyl	Ac	5	67.5 ± 1.8	5.5 ± 0.9	14.0 ± 1.1
15r	piperidyl	Ac	6	**75.1 ± 0.4**	**7.1 ± 1.7**	**12.6 ± 0.9**
15s	piperidyl	Cbz	5	16.3 ± 2.9	4.3 ± 0.6	4.9 ± 0.5
15t	piperidyl	Cbz	6	6.5 ± 2.3	7.9 ± 0.4	6.2 ± 0.7
2	H	Ac	5	29.2 ± 0.3	16.4 ± 3.2	10.3 ± 1.8
3	H	Ac	6	30.6 ± 1.1	16.1 ± 0.7	14.0 ± 1.1

183 **Table 3. IC_{50} values of representative compounds for OfHex1, HsHexB, and hOGA.**

Compd	IC_{50} (μM)		
	OfHex1	**HsHexB**	**hOGA**
11d	13.4 ± 1.2	> 100	> 100
15a	8.5 ± 0.8	> 100	> 100
15b	8.3 ± 1.0	> 100	66.9 ± 2.1
15j	9.7 ± 0.3	> 100	> 100
15m	11.4 ± 1.1	> 100	> 100
15n	10.9 ± 0.1	> 100	> 100
15q	7.6 ± 0.9	> 100	> 100
15r	**6.4 ± 0.3**	**> 100**	**> 100**
1	18.0 ± 1.4	55.1 ± 0.5	> 100

2	23.9 ± 0.9	97.5 ± 1.6	> 100
3	22.5 ± 0.2	94.2 ± 1.9	> 100

Optimization of Inhibitor 15r. The highest performing compound from the first stage, **15r**, was selected for further structural optimization. Based on structure–activity relationships, we fixed the 2-acetyl on the glycosyl moiety and selected a linker with six carbon atoms (n=6, Scheme 2). Then we replaced the 4-piperidyl group with a similar sized nitrogen-containing cycloalkane. Thus, five glycosyl-naphthalimides **15u-15y** were synthesized (Scheme 3). The synthetic route of **15u-15y** were identical to **15a-15t** and outlined in Schemes S7 and S8. The analysis of **15u-15y** against OfHex1 (Table 4) showed that the size of the nitrogen-containing cycloalkane could affect inhibitory efficiency. Shrinking the 4-piperidyl group of **15r** to 4-pyrrolyl (**15u**) enhanced the activity (IC_{50} value of 6.4 μM to 5.1μM). Enlargement of the piperidyl (**15r**) to azepanyl (**15y**) resulted in a 1-fold increase in inhibitory efficiency. Moreover, the addition of a methyl group at the 4-position of piperidyl (**15w**) led to slightly increased potency. However, changing the piperidyl group to morpholino (**15v**) or methylpiperazinyl (**15x**) decreased the potency against OfHex1, particularly for **15x**, which resulted in a significantly weakened inhibitory effect with IC_{50} value of 87.1 μM. Among these inhibitors, **15y** (IC_{50} = 3.1 μM against OfHex1, IC_{50} >100 μM against HsHexB, IC_{50} = 90.5 μM against hOGA) exhibited excellent potency and selectivity against OfHex1, confirming the correctness of our optimization strategy.

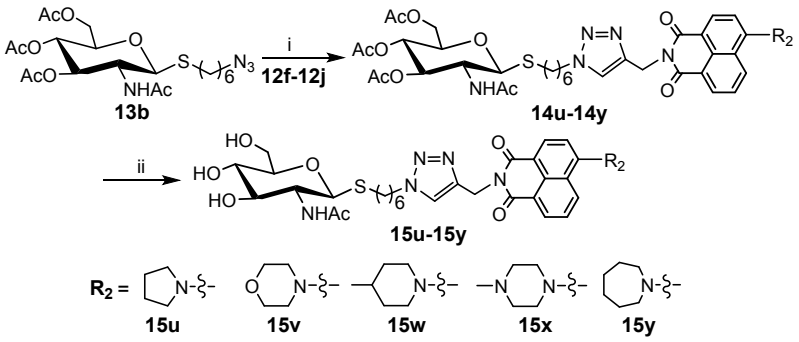

200

201 **Scheme 3.** Synthesis of glycosylated naphthalimide derivatives **15u-15y**. (i) **12f-12j**, $CuSO_4$, sodium ascorbate, THF, H_2O; (iv)

202 NH_3, MeOH.

203 **Table 4. Inhibitory activity of the optimized compounds 15u-15y against OfHex1, HsHexB, and hOGA**

Compd	R_2	IC_{50} (μM)		
		OfHex1	HsHexB	hOGA
15u		5.1 ± 0.3	> 100	68.8 ± 2.4
15v		9.4 ± 0.9	> 100	> 100
15w		6.0 ± 0.2	> 100	71.7 ± 1.9
15x		87.1 ± 3.5	> 100	7.8 ± 0.6
15y		**3.1 ± 0.4**	**> 100**	**90.5 ± 3.2**
15r		**6.4 ± 0.3**	**> 100**	**> 100**

204

205 **Further Optimization of Inhibitor 15y.** Considering that **NMAGT** bearing a methylamino on thiazoline

206 was approximately 600-fold more potent than **NGT** (bearing a methyl on thiazoline) against OfHex1[13], we
207 further attempted to modify the 2-position on glycosyl moiety of **15y** to improve its potency and selectivity.
208 Our previous experience highlighted that the large substituents at 2-position (i.e. Cbz, Table 2) would result in
209 activity loss, and so the methyl group of 2-acetamido was replaced with smaller substituents (i.e. NCH_3, CF_3,
210 Et, Pr). Accordingly, compounds **23a-23c** (Scheme 4) bearing Et, NCH_3, CF_3 and compounds **23e-23f**
211 (Scheme 5) bearing *n*-Pr and *i*-Pr were synthesized. The specific synthesis methods are shown in Schemes S9
212 and S10.

213 The inhibitory activity data of compounds **23a-23f** are exhibited in Table 5. Unfortunately, when slightly
214 increasing the size of the CH_3 group (at the 2-acetamido) to Et, $NHCH_3$, CF_3 substituents, the reduced activity
215 against OfHex1 was observed. Moreover, the larger substituents led to the lower inhibitory potency.
216 Specifically, replacement of the CH_3 to CF_3 or Et led to a 2-fold reduction in potency (from **15y** to **23c** or **23a**).
217 The loss of activity from **23a** to **23b** suggested that NH of the the $NHCH_3$ group was detrimental to the affinity
218 compared to CH_2 of the Et group at this position. When the substituent was modified from CH_3 to *n*-Pr (**23e**),
219 the inhibitory activity was reduced 10-fold. This reduction continued with *i*-Pr (**23f**) and OBn (**23d**) groups
220 leading to a loss of OfHex1 potency (IC_{50} >100 μM). Additionally, enlargement of the functional group at the
221 2-position of glycosyl moiety promoted selectivity towards OfHex1 over hOGA (compared with the IC_{50}
222 values of **15y**, **23a**, **23b**, **23c** towards hOGA), and compounds **23a-23f** showed no inhibitory potency towards
223 HsHexB.

224

225

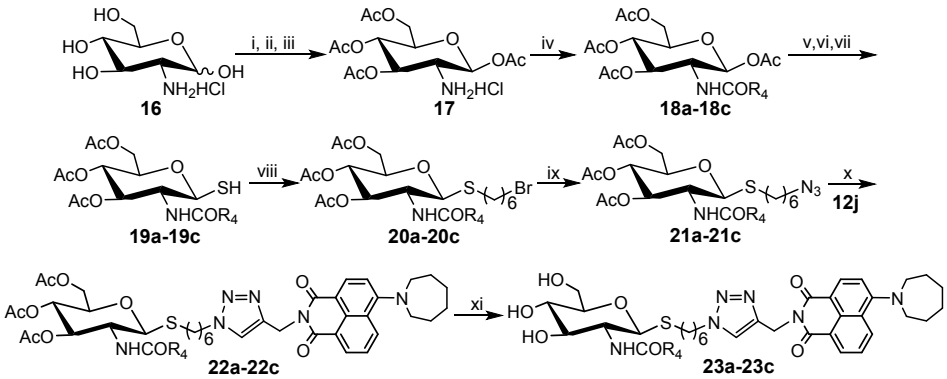

226 **23a: R_4=CH_2CH_3; 23b: R_4=$NHCH_3$; 23c: R_4=CF_3**

227 **Scheme 4.** Synthesis of glycosylated naphthalimide derivatives **23a-23e**. (i) *p*-anisaladehyde, NaOH, H_2O; (ii) Py, Ac_2O; (iii)

228 acetone, HCl, H_2O; (iv) Et_3N, CH_2Cl_2, RCOCl for **18a-18b**; Et_3N, CH_2Cl_2, TFAA for **18c**; (v) HBr, CH_3COOH, CH_2Cl_2; (vi)

229 thiourea, acetone; (vii) $Na_2S_2O_5$, CH_2Cl_2, H_2O; (viii) 1,6-dibromoalkane, K_2CO_3, acetone, H_2O; (ix) NaN_3, acetone, H_2O; (x) **12j**,

230 $CuSO_4$, sodium ascorbate, THF, H_2O; (xi) NH_3, MeOH.

231

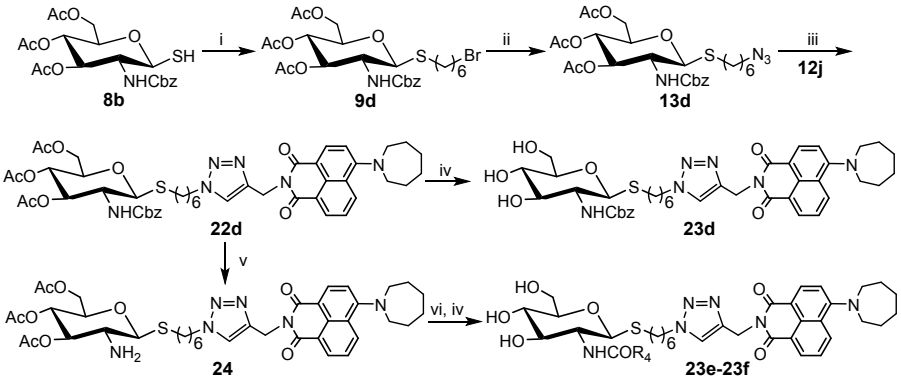

232

233 **23e: R_4=$CH_2CH_2CH_3$; 23f: R_4=$CH(CH_3)_2$**

234 **Scheme 5.** Synthesis of glycosylated naphthalimide derivatives **23d-23f**. (i) 1,6-dibromoalkane, K_2CO_3, acetone, H_2O; (ii) NaN_3,

235 acetone, H_2O; (iii) **12j**, $CuSO_4$, sodium ascorbate, THF, H_2O; (iv) NH_3, MeOH; (v) Pd/C, H_2, THF, MeOH, HCl; (vi) R_4COCl,

236 Et_3N, CH_2Cl_2, DMAP.

237

238 **Table 5. Inhibitory activity of the optimized compounds 23a-23f against OfHex1, HsHexB, and hOGA**

Compd	R_4	IC_{50} (μM)		
		OfHex1	HsHexB	hOGA
23a	**Et**	**6.8 ± 0.5**	**> 100**	**94.8 ± 0.9**
23b	$NHCH_3$	7.2 ± 0.7	> 100	97.1 ± 3.4
23c	**CF_3**	**6.4 ± 0.4**	**> 100**	**98.9 ± 1.4**
23e	*n*-Pr	30.2 ± 1.8	> 100	> 100
23f	*i*-Pr	> 100	> 100	> 100
23d	OBn	> 100	> 100	> 100
15y	**CH_3**	**3.1 ± 0.4**	**> 100**	**90.5 ± 3.2**

239

240 **Inhibitory Mechanism of Glycosylated Naphthalimides for OfHex1.** Two representative inhibitors,
241 namely **15r** and **15y**, were selected to investigate the inhibitiory mechanism of these glycosylated
242 naphthalimides. Dixon plots of **15r** and **15y** against OfHex1 were performed. As shown in Figure 2, **15r** and
243 **15y** were competitive inhibitors, with K_i values of 5.3 ± 0.2 μM and 2.7 ± 0.1 μM against OfHex1,
244 respectively.

245 To investigate the basis for the potency of these glycosylated naphthalimides towards OfHex1, the binding
246 modes of **15r**, **15y** and **23f** with OfHex1 were carried out via molecular docking. As shown in Figure 3a, the
247 glycosyl moiety from all three inhibitors was found to bind to -1 subsite of OfHex1 and the naphthalimide
248 group extended out from the active pocket. Moreover, the conformation of inhibitor **15r** was similar to that of

249 **15y** but buried shallower. For the binding mode of **23f**, the naphthalimide group had a great degree of rotation
250 compared to **15r**, which moved away from residues Gly485 and Ala486.

251 In an effort to further illustrate the appropriate binding modes of compounds **15r**, **15y** and **23f** in complex
252 with OfHex1, 30 ns MD simulations were performed (Figures 3b-3c). The root-mean-square deviations
253 (RMSD) values were maintained at around 1.5-3.1 Å for these three systems, suggesting the complexes
254 underwent reasonable conformational changes (Figure 3b). The conformations of **15r**, **15y** and **23f** combined
255 with OfHex1 at 30 ns of the MD simulations were superimposed (Figure 3c).

256 In comparison to the docking conformations (Figure 3a), the alkyl chain of **15r** and **15y** showed a high
257 degree of folding after MD simulations (Figure 3c). Thus, naphthalimide moiety of **15r** and **15y** could bind to
258 +1 subsite of the OfHex1 pocket with high affinity, forming strong π-π stacking interactions with Trp490 and
259 van der Waals interactions with Val327 (Figures 3c-3e). The glycosyl moiety of **15r** was found to bind to the
260 -1 subsite via H-bonding interactions with residues His246, Glu297, Asp299, Glu367, and the triazole ring
261 bound with residue Tyr475 at a distance of 2.1 Å (Figure 3d). These interactions in -1 subsite are much less
262 than that of PUGNAc (K_i = 0.1 μM against OfHex1)[9], which may suggest that the efficiency of these
263 glycosylated naphthalimids is in micromolar range. As a comparison, the glycosyl moiety of **15y** buried
264 shallower than **15r**, which might be due to the increased size of cycloalkane (from piperidyl to azepanyl)
265 leading to the steric hindrance in -1 subsite (Figure 3c). Accordingly, the glycosyl moiety of **15y** formed four
266 fewer hydrogen bonds than **15r** (five hydrogen bonds) with residues Arg220, Glu297, Asp299, Tyr475
267 (Figures 3d-3e). However, the triazole ring of **15y** could form three hydrogen bonds (more than **15r**) with
268 residues Trp483, val484, and Trp490 (Figures 3d-3e). On the basis of these observations, **15y** (K_i = 2.7 μM)
269 ultimately displayed a higher inhibitory potency against OfHex1 than **15r** (K_i = 5.3 μM).

It was noteworthy that the conformation of **23f** significantly differed to **15r** and **15y** (Figures 3c and 3f). In detail, the glycosyl moiety of **23f** was buried at the entrance of the OfHex1 pocket and only interacted with Arg 220, whilst the triazole bearing naphthalimide moiety extended out from the active pocket (Figure 3f). These results revealed that the branched and large *i*-Pr group led to the glycosyl moiety of **23f** being unable to move deeply into the -1 subsite of OfHex1, explaining the basis for the loss of activity.

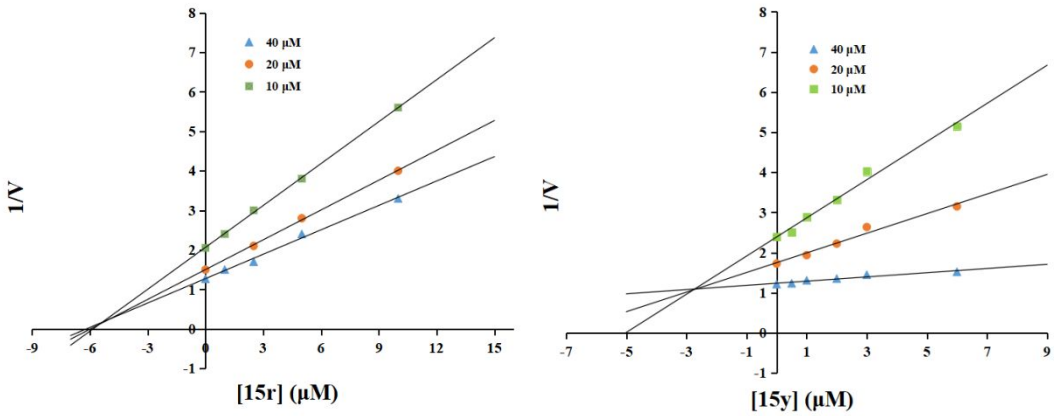

Figure 2. Dixon plots for inhibitors **15r** and **15y** against OfHex1

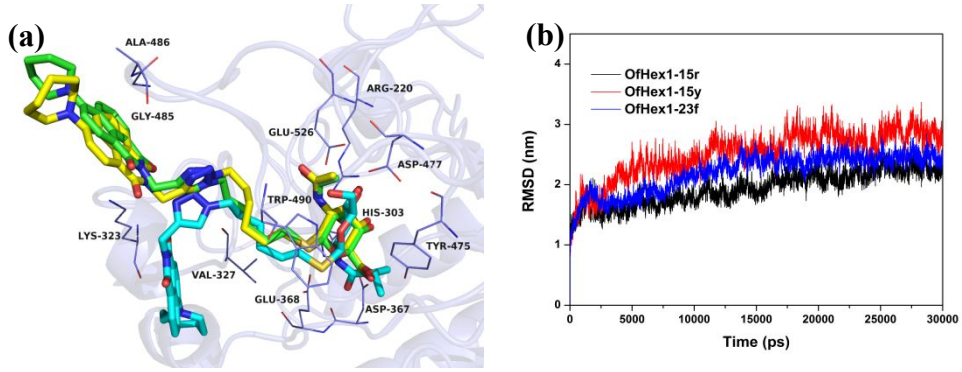

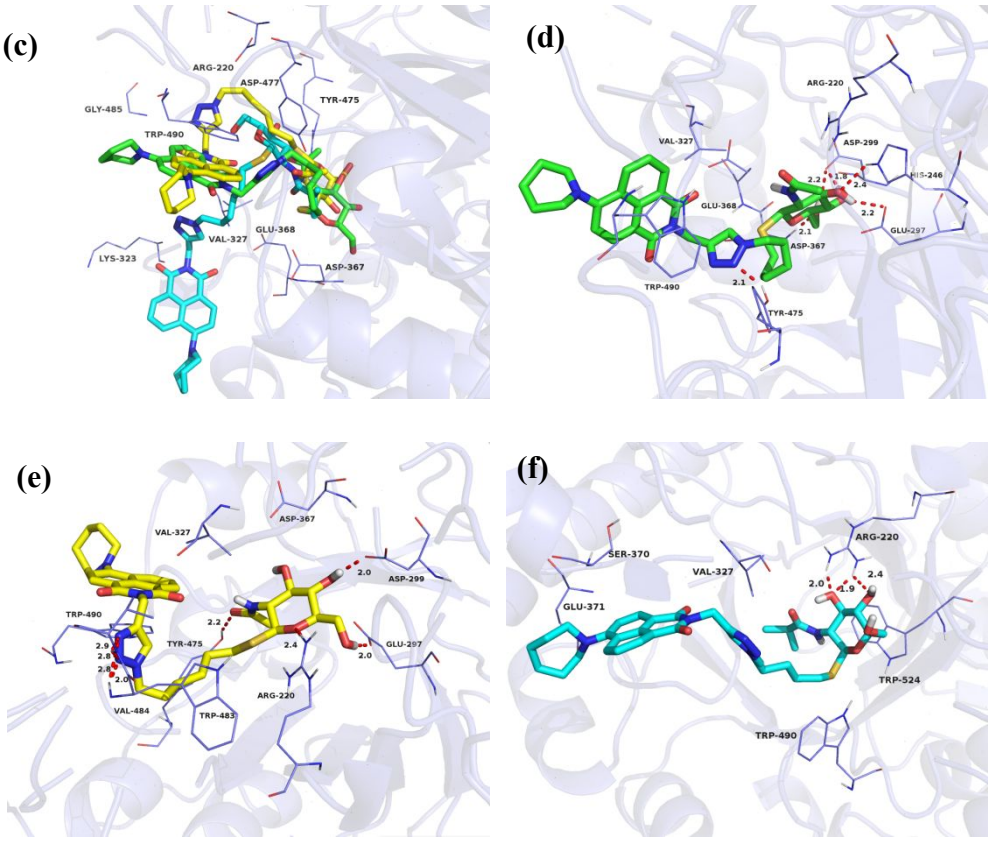

Figure 3. Binding mechanism of **15r**, **15y** and **23f** with OfHex1 revealed by molecular docking and MD simulations. (a) Molecular docking and (c) 30 ns MD simulations of OfHex1 in complex with **15r**, **15y** and **23f**. (b) RMSD changes of **15r**, **15y** and **23f** in the active pocket of OfHex1. Specific binding modes of (d) OfHex1-**15r**, (e) OfHex1-**15y**, and (f) OfHex1-**23f** systems at 30 ns after MD simulations. The protein is shown as a cartoon style. Compound **15r** is shown in green, **15y** is shown in yellow, **23f** is shown in cyan (colored according to the element).

Insecticidal Activity. The glycosylated naphthalimides that showed higher inhibitory activity against OfHex1 were further selected to evaluate their insecticidal activity. As shown in Table 6, the activity of compounds **15b** and **15y** were higher than the control drug hexaflumuron towards *Myzus persicae* with the mortalities of 41.5% and 47.2% at a concentration of 200 μg/mL. Moreover, Compounds **15m**, **15n** and **23a** displayed > 50% mortality against *Myzus persicae* at 600 μg/mL, and the remaining compounds exhibited

293 relatively weak activity. For *Plutella xylostella*, compounds **15m**, **15n**, **15r**, **15v**, **15w** and **15y** exhibited high
294 activity with mortality rates over 50% at 600 μg/mL, which were lower than those of hexaflumuron (93.3%).
295 Although many of the compounds displayed moderate or a lack of insecticidal activity against *Plutella*
296 *xylostella*, a smaller body size of the treated insects was noted after 72 hours feeding, compared to the negative
297 control groups. The structure–activity relationships of these glycosylated naphthalimides against *Myzus*
298 *persicae* and *Plutella xylostella* showed that the $N(CH_3)_2$ substituent at the 4-position of the naphthalimides
299 was perhaps the active functional group for insecticidal activity.

300

301 **Table 6. Insecticidal activity of glycosylated naphthalimides (mortality (%) ± SD).**

Compd	Myzus persicae		Plutella xylostella
	600 μg/mL	200 μg/mL	600 μg/mL
11d	46.2 ± 2.8		16.7 ± 0.9
15a	7.9 ± 0.5		33.3 ± 1.2
15b	76.7 ± 3.7	41.5 ± 0.9	23.3 ± 0.8
15j	19.6 ± 3.5		10.0 ± 0.8
15m	74.1 ± 1.1	38.8 ± 2.5	53.3 ± 1.6
15n	68.0 ± 1.7	29.4 ± 1.2	66.7 ± 2.4
15q	31.9 ± 2.5		33.3 ± 2.0
15r	48.9 ± 3.6		56.7 ± 1.2
15u	39.2 ± 0.5		13.3 ± 1.2

15v	9.5 ± 0.9		50.0 ± 0.0
15w	43.1 ± 1.3		53.3 ± 0.9
15y	82.7 ± 2.4	47.2 ± 1.9	63.3 ± 3.1
23a	55.1 ± 4.1	17.1 ± 1.7	43.3 ± 1.2
23b	39.2 ± 3.0		16.7 ± 0.4
23c	26.2 ± 0.8		20.0 ± 1.6
Hexaflumuron	75.6 ± 2.2	40.7 ± 3.1	93.3 ± 0.5

Effects of 15r and 15y on *Ostrinia furnacalis* Larvae. Compounds **15r** and **15y** were the most effective OfHex1 inhibitors observed in this study. Both compounds thus fed to 3th-instar day 1 *Ostrinia furnacalis* larvaes for 5 days. As shown in Figure 4, the larvaes of inhibitor-containing feeding groups (Figures 4c and 4d) exhibited slower growth than the control group (Figure 4b). Especially inhibitor **15y** led to the death of > 76 % of larvaes after 5 days of feeding. The *Ostrinia furnacalis* larvaes that survived had significantly reduced body sizes (Figure 4d). These results suggested that OfHex1 inhibitors are promising pest control reagents.

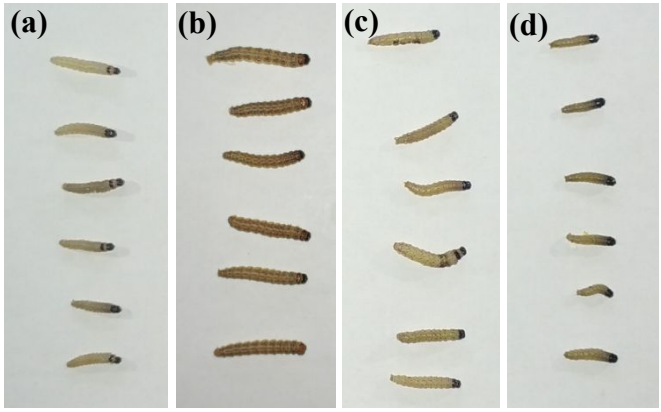

Figure 4. Bioactivity of OfHex1 inhibitors **15r** and **15y** for *Ostrinia furnacalis* larvaes. (a) 3th-instar day 1 larvaes prior to inhibitor treatment; larvaes of (b) DMSO, (c) **15r**, (d) **15y** containing diet-fed group after 5 days of feeding.

312

313 In conclusion, we present the molecular design, synthesis, and inhibitory activity against OfHex1, HsHexB,
314 and hOGA of glycosylated naphthalimides **11a-11e** and **15a-15t**. As a result, compound **15r** exhibited the
315 higher efficiency against OfHex1 with a K_i value of 5.3 μM and excellent selectivity (IC_{50} >100 μM against
316 HsHexB and hOGA). After in-depth SAR studies, an azepanyl naphthalimide derivative, compound **15y** (K_i
317 =2.7 μM against OfHex1, IC_{50} >100 μM against HsHexB, IC_{50} = 90.5 μM against hOGA), was identified as a
318 promising OfHex1 inhibitor. Moreover, molecular docking and MD simulations studies of **15r**, **15y** and **23f**
319 were performed to allow us to rationalize the basis for the potency of these glycosylated naphthalimides
320 towards OfHex1. In addition, the efficient OfHex1 inhibitors were further selected to evaluate their insecticidal
321 activity against *Myzus persicae* and *Plutella xylostella*. The results showed that compounds **15b** and **15y** had
322 higher insecticidal activity against *Myzus persicae* than the commercial pesticide hexaflumuron. Furthermore,
323 feeding experiments demonstrated that the OfHex1 inhibitors **15r** and **15y** could effectively inhibit the growth
324 of *Ostrinia furnacalis* larvae. Thus, the structure−activity relationships combined with docking and MD
325 simulations studies provide direction for the further structural optimization for OfHex1, and the development
326 of green pest control and management agents.

327

328 ASSOCIATED CONTENT

329 **■ Supporting Information**

330 Experimental procedures, Molecular docking and MD simulations results, ^{1}H NMR and ^{13}C NMR spectrum.

331 **■ AUTHOR INFORMATION**

Corresponding Author

*E-mail: zhangjianjun@cau.edu.cn.

*E-mail: qingyang@dlut.edu.cn.

Author Contributions

[#]These authors contributed equally to this work. All authors have given approval to the final version of the manuscript.

Notes

The authors declare no competing financial interest.

■ ACKNOWLEDGMENTS

We acknowledge the financial support by the National Natural Science Foundation (21772230, 31425021), and Chinese Universities Scientific Fund (No.2019TC135).

■ ABBREVIATIONS

GH18, glycoside hydrolase family 18; GH20, glycoside hydrolase family 20; MD, molecular dynamics.

REFERENCES

1. Sutherland, T. E.; Andersen, O. A.; Betou, M.; Eggleston, I. M.; Maizels, R. M.; van Aalten, D.; Allen, J. E., Analyzing airway inflammation with chemical biology: dissection of acidic mammalian chitinase function with a selective drug-like Inhibitor. *Chem. Biol.* **2011,** *18* (5), 569-579.

2. Merzendorfer, H.; Zimoch, L., Chitin metabolism in insects: structure, function and regulation of chitin synthases and chitinases. *J. Exp. Biol.* **2003,** *206* (24), 4393-4412.

3. Liu, J.; Liu, M.; Yao, Y.; Wang, J.; Li, Y.; Li, G.; Wang, Y., Identification of novel potential β-N-acetyl-D-hexosaminidase

353 inhibitors by virtual screening, molecular dynamics simulation and MM-PBSA calculations. *Int. J. Mol. Sci.* **2012,** *13*,
354 4545-4563.

355 4. Dahiya, N.; Tewari, R.; Hoondal, G. S., Biotechnological aspects of chitinolytic enzymes: a review. *Appl. Microbiol.*
356 *Biotechnol.* **2006,** *71* (6), 773-782.

357 5. Liu, T.; Chen, L.; Ma, Q.; Shen, X.; Yang, Q., Structural insights into chitinolytic enzymes and inhibition mechanisms of
358 selective inhibitors. *Current Pharmaceutical Design* **2014,** *20* (5), 754-770.

359 6. Zhu, K. Y.; Merzendorfer, H.; Zhang, W.; Zhang, J.; Muthukrishnan, S., Biosynthesis, turnover, and functions of chitin in
360 insects. *Annu. Rev. Entomol.* **2016,** *61*, 177-196.

361 7. Chen, L.; Liu, T.; Duan, Y.; Lu, X.; Yang, Q., Microbial secondary metabolite, Phlegmacin B-1, as a novel inhibitor of insect
362 chitinolytic enzymes. *J. Agric. Food Chem.* **2017,** *65* (19), 3851-3857.

363 8. Dong, Y.; Jiang, X.; Liu, T.; Ling, Y.; Yang, Q.; Zhang, L.; He, X., Structure-based virtual screening, compound synthesis,
364 and bioassay for the design of chitinase inhibitors. *J. Agric. Food Chem.* **2018,** *66* (13), 3351-3357.

365 9. Liu, T.; Zhang, H.; Liu, F.; Chen, L.; Shen, X.; Yang, Q., Active-pocket size differentiating insectile from bacterial chitinolytic
366 β-N-acetyl-D-hexosaminidases. *Biochem. J.* **2011,** *438* (3), 467-474.

367 10. Yang, H.; Liu, T.; Qi, H.; Huang, Z.; Hao, Z.; Ying, J.; Yang, Q.; Qian, X., Design and synthesis of thiazolylhydrazone
368 derivatives as inhibitors of chitinolytic N-acetyl-β-D-hexosaminidase. *Bioorg Med Chem* **2018,** *26* (20), 5420-5426.

369 11. Yang, Q.; Liu, T.; Liu, F.; Qu, M.; Qian, X., A novel β-N-acetyl-D-hexosaminidase from the insect Ostrinia furnacalis
370 (*Guenee*). *FEBS J* **2008,** *275* (22), 5690-702.

371 12. Liu, T.; Zhang, H.-T.; Liu, F.-Y.; Wu, Q.-Y.; Shen, X.; Yang, Q., Structural determinants of an insect
372 β-N-acetyl-D-hexosaminidase specialized as a chitinolytic enzyme. *J. Biol. Chem.* **2011,** *286* (6), 4049-4058.

373 13. Liu, T.; Xia, M.; Wang, J.; Zhang, H.; Shen, X.; Zhou, H.; Yang, Q., Exploring NAG-thiazoline and its derivatives as
374 inhibitors of chitinolytic β-acetylglucosaminidases. *FEBS Lett* **2015,** *589* (1), 110-6.

375 14. Liu, T.; Guo, P.; Zhou, Y.; Wang, J.; Chen, L.; Yang, H.; Qian, X.; Yang, Q., A crystal structure-guided rational design
376 switching non-carbohydrate inhibitors' specificity between two β-GlcNAcase homologs. *Sci. Rep.* **2014,** *4*, 6188.

377 15. Chen, W.; Shen, S.; Dong, L.; Zhang, J.; Yang, Q., Selective inhibition of β-N-acetylhexosaminidases by
378 thioglycosyl-naphthalimide hybrid molecules. *Bioorg. Med. Chem.* **2018,** *26* (2), 394-400.

379 16. Duan, Y.; Liu, T.; Zhou, Y.; Dou, T.; Yang, Q., Glycoside hydrolase family 18 and 20 enzymes are novel targets of the
380 traditional medicine berberine. *J. Biol. Chem.* **2018,** *293* (40), 15429-15438.

381 17. Shen, S.; Chen, W.; Dong, L.; Yang, Q.; Lu, H.; Zhang, J., Design and synthesis of naphthalimide group-bearing
382 thioglycosides as novel β-N-acetylhexosaminidases inhibitors. *J. Enzyme Inhib. Med. Chem.* **2018,** *33* (1), 445-452.

383 18. Shen, S.; Dong, L.; Chen, W.; Zeng, X.; Lu, H.; Yang, Q.; Zhang, J., Modification of the thioglycosyl-naphthalimides as
384 potent and selective human O-GlcNAcase inhibitors. *Acs Med. Chem. Lett.* **2018,** *9* (12), 1241-1246.

385 19. Kong, H.; Lu, H.; Dong, Y.; Liang, X.; Jin, S.; Chen, W.; Liu, T.; Yang, Q.; Zhang, J., Synthesis of NAM-thiazoline

386 derivatives as novel O-GlcNAcase inhibitors. *Carbohydr Res* **2016,** *429*, 54-61.

387 20. SYBYL Molecular Modeling Software, 7.3, 2006, Tripos, St. Louis, MO.

388 21. Jain, A. N.; Scoring noncovalent protein–ligand interactions: a continuous differentiable function tuned to compute binding
389 affinities. *J. Comput. Aided. Mol. Des*. **1996**, *10*, 427–440.

390 22. Welch, W.; Ruppert J.; Jain, A. N.; Hammerhead: fast, fully automated docking of flexible ligands to protein binding sites.
391 *Chem. Biol*. **1996**, *3*, 449–462.

392 23. Clark, R. D.; Strizhev, A.; Leonard, J. M.; Blake, J. F.; Matthew, J. B.; Consensus scoring for ligand/protein interactions. *J.*
393 *Mol. Graph. Model*. **2002**, *20*, 281–295.

394 24. Case DA, Babin V, Berryman JT, Betz RM, Cai Q, Cerutti DS, Cheatham III TE, Darden TA, Duke RE, Gohlke H, Goetz
395 AW, Gusarov S, Homeyer N, Janowski P, Kaus J, Kolossváry I, Kovalenko A, Lee TS, LeGrand S, Luchko T, Luo R, Madej B,
396 Merz KM, Paesani F, Roe DR, Roitberg A, Sagui C, Salomon-Ferrer R, Seabra G, Simmerling CL, Smith W, Swails J, Walker
397 RC, Wang J, Wolf RM, Wu X, Kollman PA. **2014**, AMBER 14. University of California, San rancisco

398 25. Duan, Y.; Wu, C.; Chowdhury, S.; Lee, M. C.; Xiong, G.; Zhang, W.; Yang, R.; Cieplak, P.; Luo, R.; Lee, T.; Caldwell, J.;
399 Wang, J.; Kollman, P., A point-charge force field for molecular mechanics simulations of proteins based on condensed-phase
400 quantum mechanical calculations. *J. Comput. Chem.* **2003,** *24*, 1999-2012.

401 26. Wang, J.; Wolf, R. M.; Caldwell, J. W.; Kollman, P. A.; Case, D. A., Development and testing of a general amber force field.
402 *J. Comput. Chem.* **2004,** *26*, 114.

403 27. Darden, T.; York, D.; Pedersen, L., Particle mesh Ewald: An N·log(N) method for Ewald sums in large systems. *J. Chem.*
404 *Phys.* **1993,** *98*, 10089-92.

405 28. Ryckaert, J. P.; Ciccotti, G.; Berendsen, H. J. C., Numerical integration of the Cartesian equations of motion of a system with
406 constraints: molecular dynamics of n-alkanes. *J. Comput. Phys.* **1977,** *23*, 327-41.

407 29. Sun, G.; Zhang, J.; Jin, S.; Zhang, J., Synthesis and insecticidal activities of 5-deoxyavermectin B2a oxime ester derivatives.
408 *RSC Adv.* **2018,** *8* (7), 3774-3781.

409 30. Sun, G.-S.; Xu, X.; Jin, S.-H.; Lin, L.; Zhang, J.-J., Ovicidal and insecticidal activities of pyriproxyfen derivatives with an
410 oxime ester group. *Molecules* **2017,** *22* (6), 958/1-958/11.

411 31. Guo, P.; Chen, Q.; Liu, T.; Xu, L.; Yang, Q.; Qian, X., Development of unsymmetrical dyads as potent
412 noncarbohydrate-based inhibitors against human β-N-Acetyl-D-hexosaminidase. *ACS Med. Chem. Lett.* **2013,** *4* (6), 527-531.

413 32. Berchel, M.; Haelters, J.-P.; Couthon-Gourves, H.; Deschamps, L.; Midoux, P.; Lehn, P.; Jaffres, P.-A., Modular construction
414 of fluorescent lipophosphoramidates by Click Chemistry. *Eur. J. Org. Chem.* **2011,** (31), 6294-6303.

415 33. Berchel, M.; Haelters, J.-P.; Couthon-Gourves, H.; Deschamps, L.; Midoux, P.; Lehn, P.; Jaffres, P.-A., Modular construction
416 of fluorescent lipophosphoramidates by Click Chemistry. *Eur. J. Org. Chem.* **2011,** *2011* (31), 6294-6303.

417

418 **Graphic for table of contents**

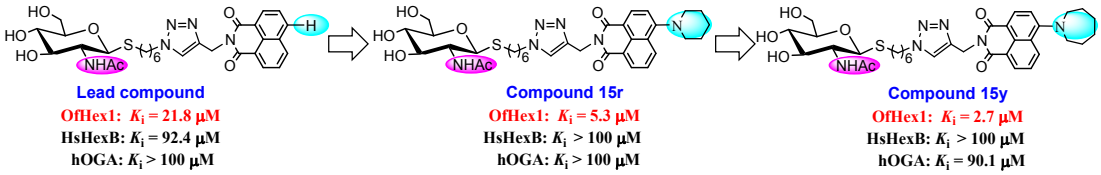

419